PNNL-21962

U.S. DEPARTMENT OF ENERGY

Prepared for the U.S. Department of Energy
under Contract DE-AC05-76RL01830

Potential Detections of ^{133}Xe Released from ANSTO Facilities Using IMS Samplers

Paul W. Eslinger
Brian T. Schrom
Rosara F. Kephart
Harry S. Miley

September 2012

Pacific Northwest
NATIONAL LABORATORY

DISCLAIMER

This report was prepared as an account of work sponsored by an agency of the United States Government. Neither the United States Government nor any agency thereof, nor Battelle Memorial Institute, nor any of their employees, makes **any warranty, express or implied, or assumes any legal liability or responsibility for the accuracy, completeness, or usefulness of any information, apparatus, product, or process disclosed, or represents that its use would not infringe privately owned rights**. Reference herein to any specific commercial product, process, or service by trade name, trademark, manufacturer, or otherwise does not necessarily constitute or imply its endorsement, recommendation, or favoring by the United States Government or any agency thereof, or Battelle Memorial Institute. The views and opinions of authors expressed herein do not necessarily state or reflect those of the United States Government or any agency thereof.

PACIFIC NORTHWEST NATIONAL LABORATORY
operated by
BATTELLE
for the
UNITED STATES DEPARTMENT OF ENERGY
under Contract DE-AC05-76RL01830

Printed in the United States of America

Available to DOE and DOE contractors from the
Office of Scientific and Technical Information,
P.O. Box 62, Oak Ridge, TN 37831-0062;
ph: (865) 576-8401
fax: (865) 576-5728
email: reports@adonis.osti.gov

Available to the public from the National Technical Information Service,
U.S. Department of Commerce, 5285 Port Royal Rd., Springfield, VA 22161
ph: (800) 553-6847
fax: (703) 605-6900
email: orders@ntis.fedworld.gov
online ordering: http://www.ntis.gov/ordering.htm

This document was printed on recycled paper.
(9/2003)

PNNL-21962

Potential Detections of ^{133}Xe Released from ANSTO Facilities Using IMS Samplers

Paul W. Eslinger
Brian T. Schrom
Rosara F. Kephart
Harry S. Miley

September 2012

Prepared for
the U.S. Department of Energy
under Contract DE-AC05-76RL01830

Pacific Northwest National Laboratory
Richland, Washington 99352

ABSTRACT

The Australian Nuclear Science and Technology Organization (ANSTO) operates a reactor and a medical isotope production facility in Lucas Heights, Australia. Example atmospheric transport runs using historical releases from the facility illustrate that ^{133}Xe will routinely be detected at low levels at regional IMS sampling locations given the current detection limits. This observation matches with historical records of ^{133}Xe detections.

.

Contents

1.0 Introduction 7
1.1 Background 7
1.2 Purpose 8
2.0 Data 9
2.1 ANSTO Release Data 9
2.2 IMS Data 11
3.0 Model and Results 14
3.1 Atmospheric Transport Model 14
3.2 Predicted Concentrations Using ANSTO Releases 15
3.3 Analysis of Alternate Arrival Times 21
3.4 Other Potential Source Terms 24
3.5 Detailed Analysis of One Short Detection Sequence 29
4.0 Isotopic Analysis of ANSTO Stack Releases 32
5.0 Summary 36
6.0 References 37

Tables

Table 1. Probabilities of model-measurement detection agreements for the IMS station (AUX04) in Melbourne, Australia. 23
Table 2. Comparison of the percent of days measured and modeled concentrations of 133Xe are above specified concentrations at three southern hemisphere IMS noble gas samplers. 29
Table 3. Comparison of measured and modeled concentrations of ^{133}Xe at Melbourne (AUX04) for releases from ANSTO facilities between 12/9/2008 and 12/12/2008. 30
Table 4. Isotopic structure of Xe using 30 clusters for the 15-minute data ANSTO release data. 32
Table 5. Example isotopic information for the five Xe clusters for the 30-cluster analysis of the 15-minute data ANSTO release data. 33
Table 6. Example time ordering of releases of cluster means based on ^{133}Xe/^{135}Xe ratios for the 30-cluster analysis of the 15-minute data ANSTO release data. 34

Figures

Figure 1. IMS Radionuclide Sampling Locations that Collect Noble Gases. 7

Figure 2. IMS Radionuclide Sampling Locations that Collect Particulate Data.....8

Figure 3. Daily releases of ^{133}Xe from Building 54 at ANSTO from November 2008 through April 2012. 9

Figure 4. Daily releases of ^{133}Xe from Building 54 at ANSTO for April through August 2011. 10

Figure 5. Releases of ^{133}Xe from Building 54 at ANSTO on 15-Minute intervals for January 11 and 12, 2010.....11

Figure 6. Measured ^{133}Xe Concentrations from the IMS noble gas sampler (AUX04) at Melbourne, Australia, since August 2009.....12

Figure 7. Measured ^{133}Xe Concentrations from the IMS noble gas sampler (AUX09) at Darwin, Australia, since August 2009. 12

Figure 8. Measured ^{133}Xe Concentrations from the IMS noble gas sampler (NZX46) at Chatham Island, New Zealand, since August 2009.....13

Figure 9. Modeled ^{133}Xe concentrations ten days after a release of 3.18×10^{13} Bq on November 2, 2010, from the ANSTO facilities. No radioactive decay is used. 15

Figure 10. Percent of days that modeled ^{133}Xe concentrations were above 0.3 mBq/m^3 at IMS locations with noble gas samplers given the historical releases from the ANSTO facilities....16

Figure 11. Percent of days that modeled ^{133}Xe concentrations were above 0.3 mBq/m^3 at all IMS radionuclide locations given the historical releases from the ANSTO facilities. 16

Figure 12. Time history of modeled and sampled concentrations for the IMS station (AUX04) in Melbourne, Australia, given the ^{133}Xe historical releases from the ANSTO facilities. 17

Figure 13. Comparison of modeled concentrations with sampled concentrations for the IMS station (AUX04) in Melbourne, Australia, given the ^{133}Xe historical releases from the ANSTO facilities. 18

Figure 14. Time history of modeled and sampled concentrations for the IMS station (AUX09) in Darwin, Australia, given the ^{133}Xe historical releases from the ANSTO facilities.....19

Figure 15. Comparison of modeled concentrations with sampled concentrations for the IMS station (AUX09) in Darwin, Australia, given the ^{133}Xe historical releases from the ANSTO facilities.....19

Figure 16. Time history of modeled and sampled concentrations for the IMS station (NZX46) in Chatham Island, New Zealand, given the ^{133}Xe historical releases from the ANSTO facilities.....20

Figure 17. Comparison of modeled concentrations with sampled concentrations for the IMS station (NZX46) in Chatham Island, New Zealand, given the ^{133}Xe historical releases from the ANSTO facilities. 21

Figure 18. Best neighbor analysis with time offset for concentrations for the IMS station (AUX04) in Melbourne, Australia, given the ^{133}Xe historical releases from the ANSTO facilities.....22

Figure 19. Binary matching results for offset for concentrations for the IMS station (AUX04) in Melbourne, Australia. Left pane provided same day results. Right pane shows nearest neighbor results.....22

Figure 20. Successful detection predictions of same day model results versus closest neighbor data for the three IMS noble gas stations closest to the ANSTO facilities. 23

Figure 21. Successful non-detection predictions of same day model results versus closest neighbor data for the three IMS noble gas stations closest to the ANSTO facilities. 24

Figure 22. Worldwide nuclear power plant locations and southern hemisphere medical isotope production facilities. 25

Figure 23. Time history of modeled and sampled concentrations for the IMS station (AUX04) in Melbourne, Australia, given the ^{133}Xe historical releases from the ANSTO facilities and estimated releases from Argentina, South Africa and Indonesia. 26

Figure 24. Comparison of modeled concentrations with sampled concentrations for the IMS station (AUX04) in Melbourne, Australia, given the ^{133}Xe historical releases from the ANSTO facilities and estimated releases from Argentina, South Africa and Indonesia. 27

Figure 25. Time history of modeled and sampled concentrations for the IMS station (AUX09) in Darwin, Australia, given the ^{133}Xe historical releases from the ANSTO facilities..... 28

Figure 26. Comparison of measured and modeled concentrations of ^{133}Xe at Melbourne (AUX04) for releases from ANSTO facilities between 12/9/2008 and 12/12/2008. 31

Figure 27. Comparison of estimated release quantities with stack release data for ANSTO facilities between 12/9/2008 and 12/12/2008. 31

Figure 28. Cluster transitions for three isotopes of Xe using 30 clusters for the 15-minute data ANSTO release data. 35

1.0 Introduction

1.1 Background

The Comprehensive Nuclear-Test-Ban Treaty (CTBT) was adopted by the United Nations General Assembly on September 10, 1996 (CTBT 1996). The CTBT bans all States Parties (countries ratifying the treaty) from carrying out nuclear explosions. Within the CTBT the International Monitoring System (IMS) was defined to monitor the world for nuclear Explosions (CTBTO 2011). The IMS contains four primary monitoring technologies: radionuclide, seismic, hydroacoustic, and infrasound. A number of radionuclides detectable by equipment deployed by the IMS are produced for pharmaceutical purposes as well as being produced by nuclear explosions. Understanding the occurrence of detections of ^{133}Xe associated with radiopharmaceuticals is important when trying to determine whether a potentially small nuclear explosion has occurred.

The CTBT identifies 80 radionuclide sampling locations around the globe (although station 35 is not assigned coordinates in the treaty). Not all stations have yet been built. Of the 80 stations, half sample both particulates and noble gases and the others only sample particulates. The IMS station locations where noble gas sampling occurs are shown in Figure 1. Since the start of 2011, radionuclide sampling data for noble gases have been received from 27 different locations. These locations are labeled as active in Figure 1. The ANSTO facilities are about 700 km northeast of the IMS station denoted by AUX04 and they are about 15 km from the coast.

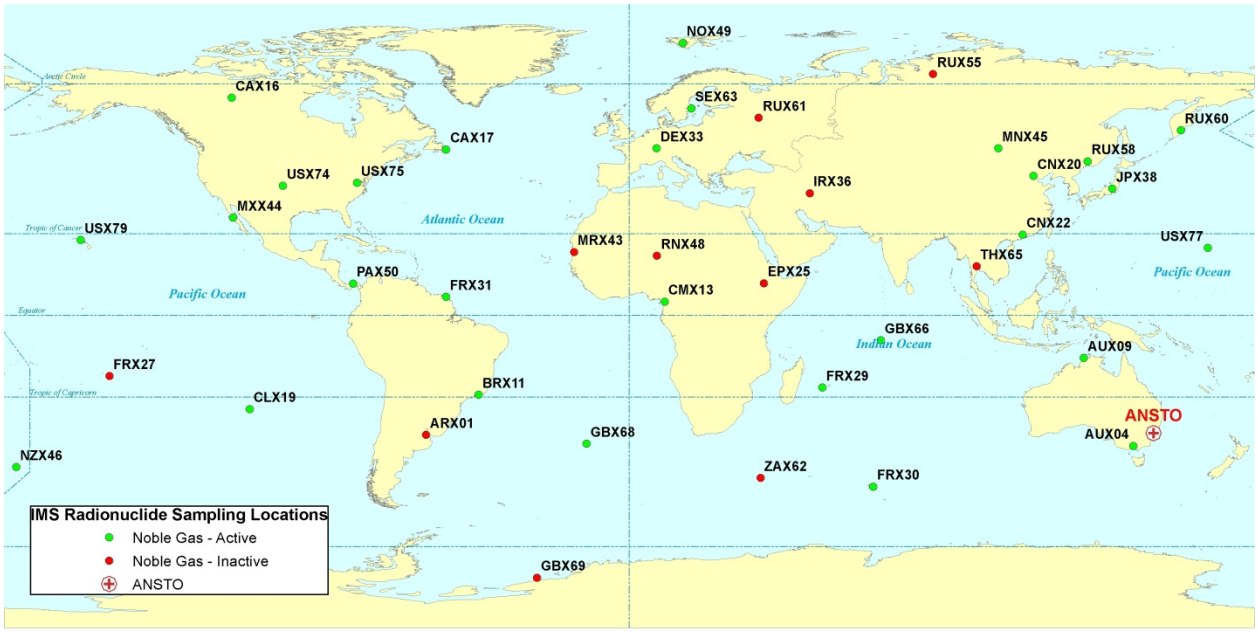

Figure 1. IMS Radionuclide Sampling Locations that Collect Noble Gases.

The suite of 80 radionuclide sampling locations in the IMS is provided in Figure 2. Although many of these locations do not have noble gas samplers, this figure is included to assist in understanding the extent of the area where releases of ^{133}Xe from ANSTO facilities potentially reach detectable concentrations.

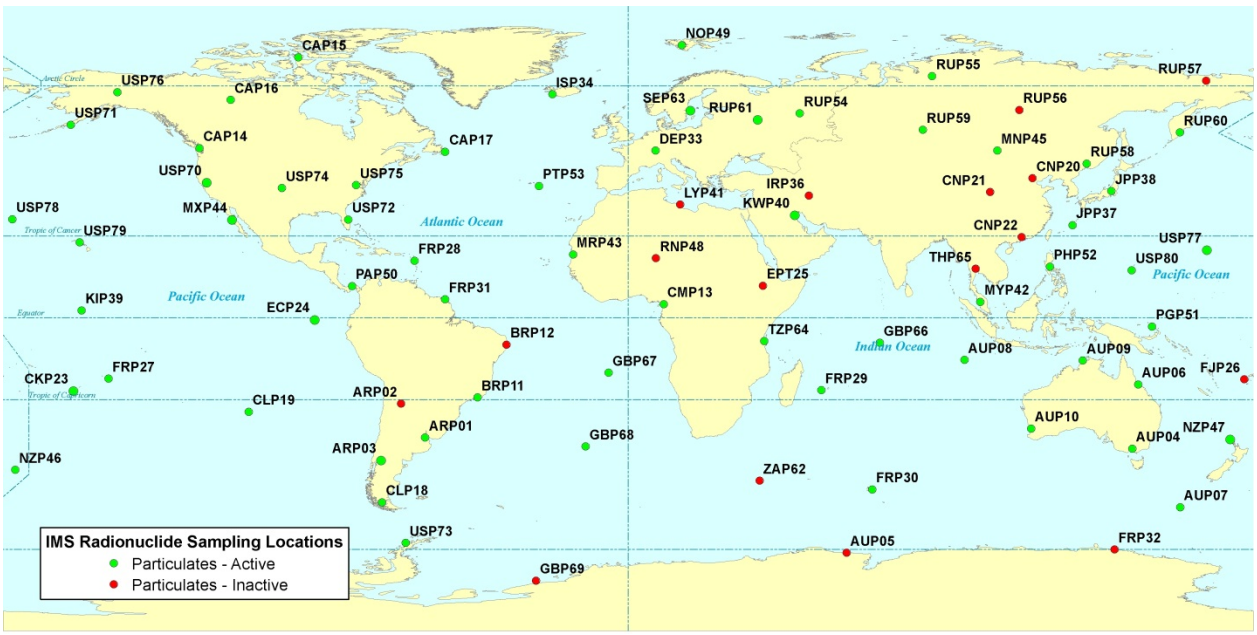

Figure 2. IMS Radionuclide Sampling Locations that Collect Particulate Data.

1.2 Purpose

Some medical isotope facilities produce enough ^{133}Xe that the releases can be detected by noble gas samplers operated for the CTBTO (Saey 2009; Saey et al. 2010; Wotawa et al. 2010; Matthews et al. 2012; Matthews et al. 2010). This paper examines the historical releases of ^{133}Xe produced in the Opal research reactor in Lucas Heights, Australia, from the perspective of potential detections in IMS samplers. The reactor is owned and operated by the Australian Nuclear Science and Technology Organization (ANSTO 2012).

2.0 Data

2.1 ANSTO Release Data

Daily releases of ^{133}Xe from Building 54 of ANSTO[1] are provided in Figure 3. The data set extends from November of 2008 to early 2012. The start of this data set coincides with the start of operation of new isotope production facilities. The average daily release since the start of 2010 is about 1.25×10^{12} Bq. Daily releases for the period April through August 2011 are shown in Figure 4. The data in this figure indicate an operational pattern that repeats on approximately a monthly cycle.

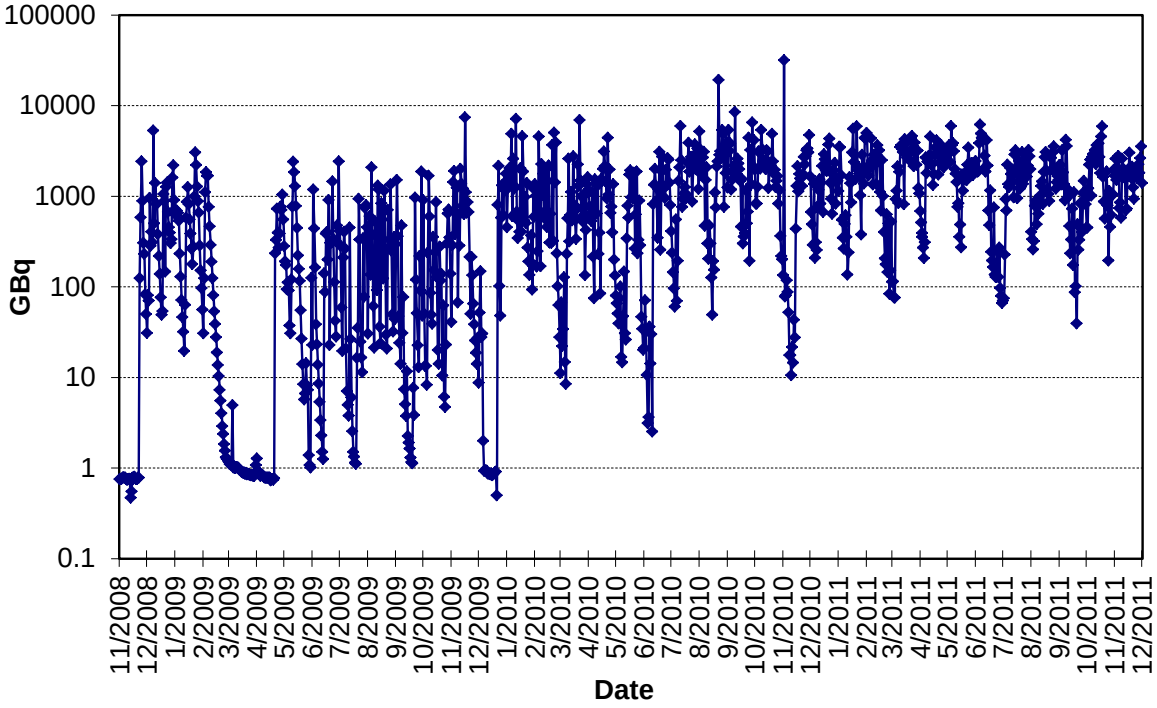

Figure 3. Daily releases of ^{133}Xe from Building 54 at ANSTO from November 2008 through April 2012.

[1] Unpublished data.

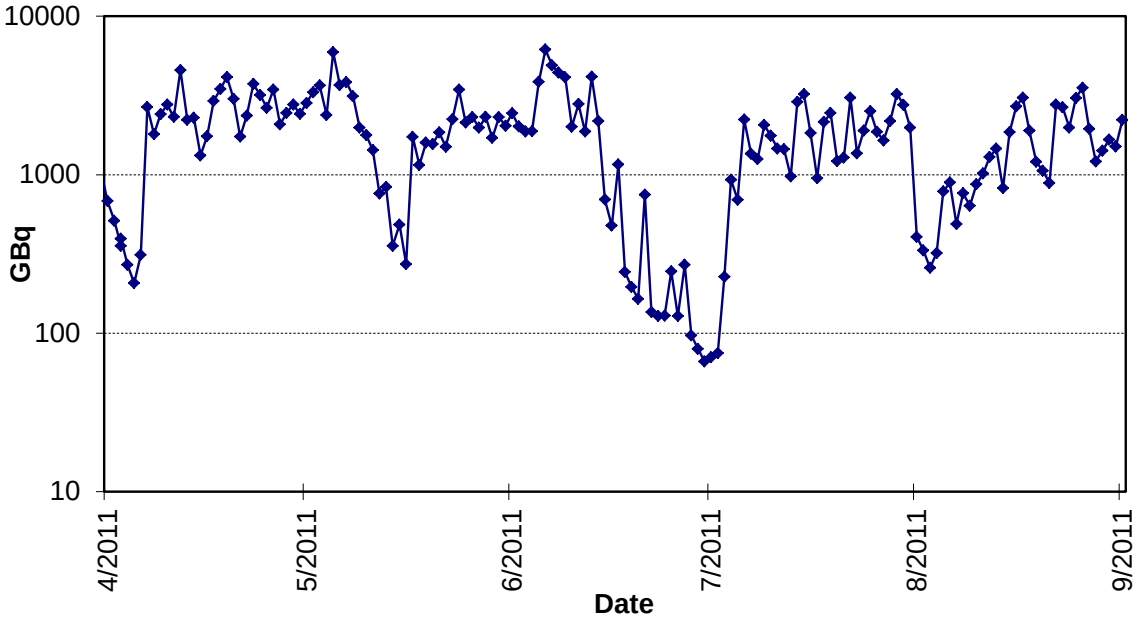

Figure 4. Daily releases of ^{133}Xe from Building 54 at ANSTO for April through August 2011.

The base data set also contains release data on contiguous 15 minute time intervals. An example plot over a two day interval in in January, 2010 is provided in Figure 5. The releases vary substantially throughout the day.

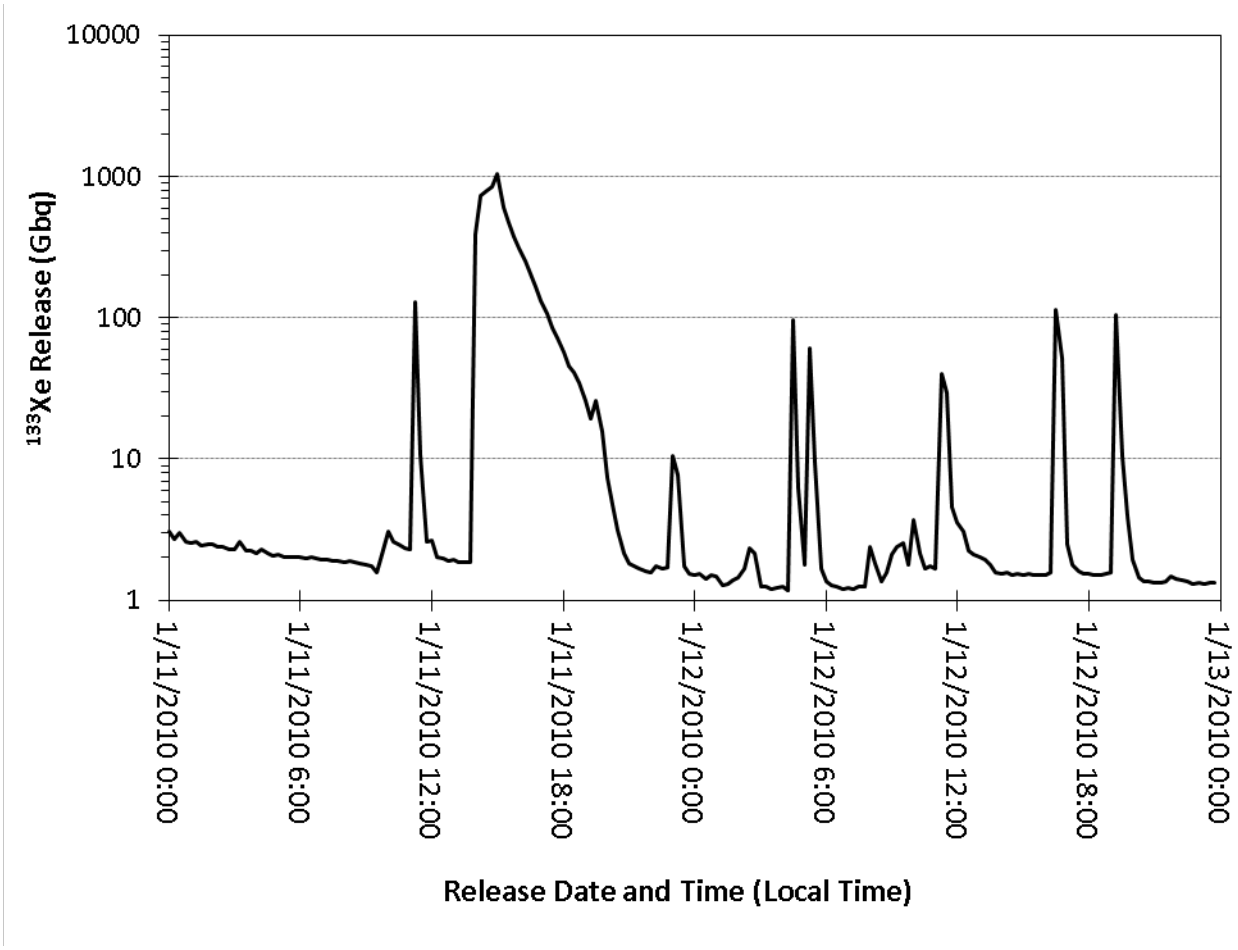

Figure 5. Releases of ^{133}Xe from Building 54 at ANSTO on 15-Minute intervals for January 11 and 12, 2010.

2.2 IMS Data

Although noble gas samplers in the IMS have been operating for a longer period of time, for this analysis we examine only the data collected since the end of August, 2009. The time limitation is applied only because we have electronic copies of the data from that time forward that were archived for other analysis purposes. We show the detection data graphically for the three IMS stations closest to the ANSTO facilities that collect noble gas data. These three stations are denoted by the following labels: AUX04, AUX09, and NZX46. None of the stations have 100% data availability for this time period. We plot all concentrations at or above 0.1 mBq/m^3 even if the concentration is not above the minimum detectable concentration.

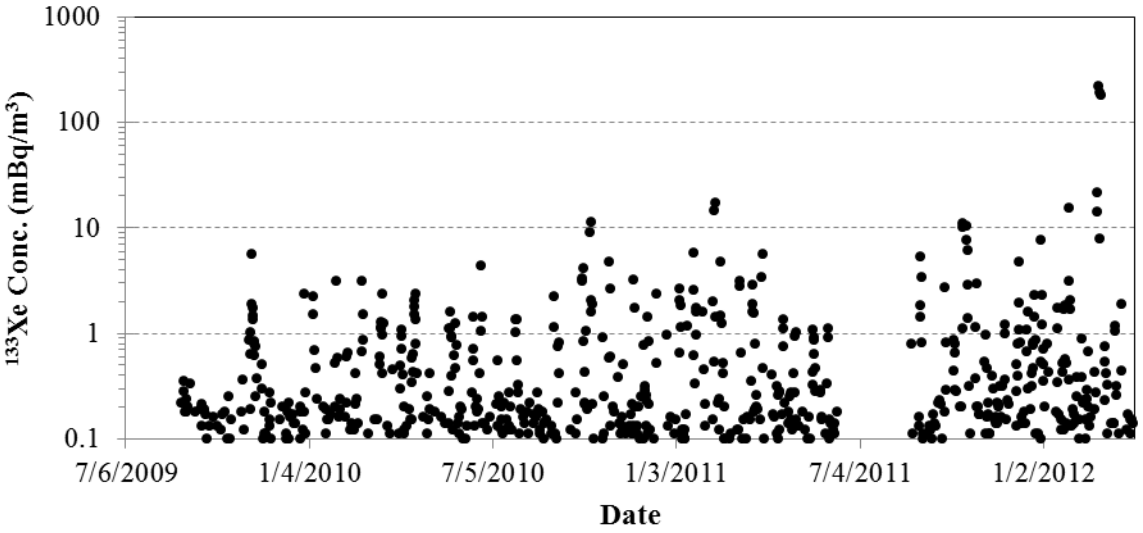

Figure 6. Measured ^{133}Xe Concentrations from the IMS noble gas sampler (AUX04) at Melbourne, Australia, since August 2009.

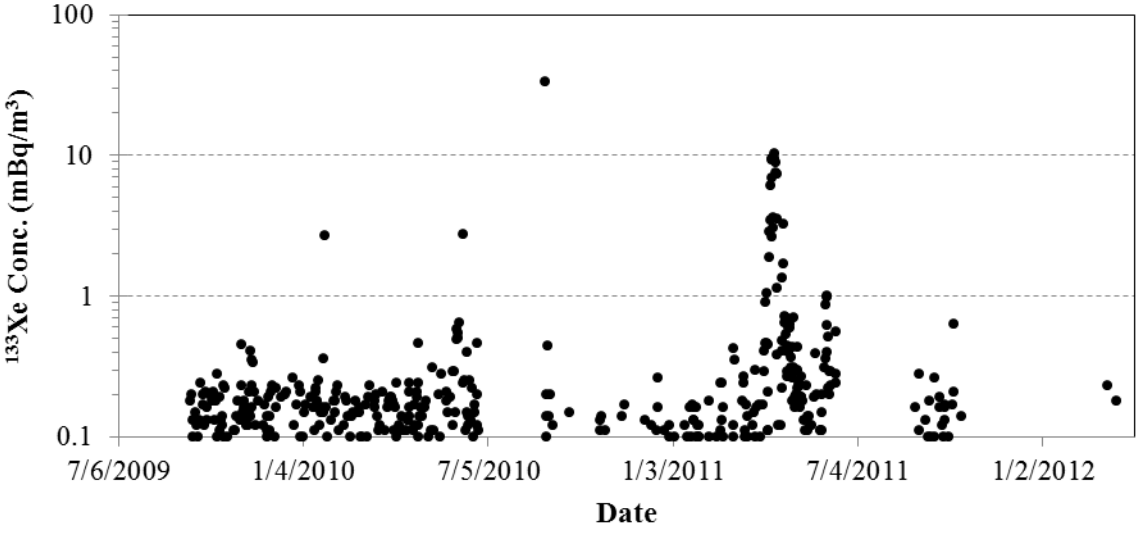

Figure 7. Measured ^{133}Xe Concentrations from the IMS noble gas sampler (AUX09) at Darwin, Australia, since August 2009.

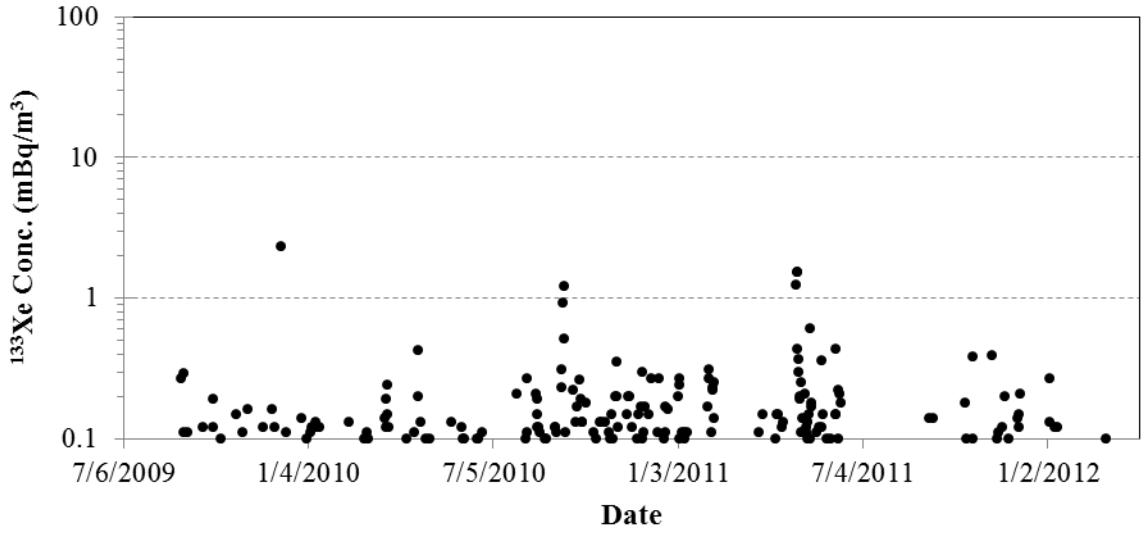

Figure 8. Measured ^{133}Xe Concentrations from the IMS noble gas sampler (NZX46) at Chatham Island, New Zealand, since August 2009.

The minimum detectable concentration (MDC) for ^{133}Xe depends on the type of sampler, the amount of air that is processed, and a number of other conditions. Using information from 4,892 sample analyses from these three stations (AUX04, AUX09 and NZX46) and the station GBX68 from September 2009 through April 2012, 95% of the calculated MDC's for ^{133}Xe were in the range 0.12 to 0.3 mBq/m^3, with a median value of 0.16 mBq/m^3. Data sets with the amount of extracted xenon below 0.3 or above 1.5 cc's were eliminated for exploring the effective MDC. In addition, a few data sets with negative, but large magnitude, estimates of ^{133}Xe concentrations were eliminated.

3.0 Model and Results

3.1 Atmospheric Transport Model

The general approach for this analysis occurs in two basic steps. First, we insert the a unit source term of ^{133}Xe in an atmospheric transport model (ATM) and run the model for 21 days of transport. The concentration fields from the individual ATM runs are then superimposed, scaled and decay corrected to yield daily concentration estimates. Finally, we compare the daily concentration estimates with the sampled data.

We modeled atmospheric transport of ^{133}I using the Hybrid Single Particle Lagrangian Integrated Trajectory (HYSPLIT) model, parallel version 4.9, maintained by the U.S. National Oceanographic and Atmospheric Administration (Draxler and Hess 1998; HYSPLIT 2011). We used three-hour archived meteorological data on a 1° grid produced for the U.S. National Weather Service's National Centers for Environmental Prediction. The archived meteorological data are available for use in the HYSPLIT model via download from a web server (GDAS 2012).

We used the particle tracking mode of the HYSPLIT code. The particle tracking mode transports a user specified number of representative particles, each released at a specific location and time, and tracks the position of each particle over time. The transport runs were performed on a 168 compute-node Linux cluster. The model used a 0.5° latitude by 0.5° longitude transport grid and 1 million particles. The simulated radionuclide activity was injected into the lower 20 meters of the atmospheric column at latitude 34.0511°S and longitude 150.9786 °E. Model concentrations at sampling locations were averaged over the bottom 100 meters of the atmospheric column. The top of the 23-layer atmospheric model domain reached 10,000 m above ground level. No atmospheric deposition was used and radioactive decay was applied in the post processing step of superimposing plumes released on different days.

To show the potential extent of the migration of ^{133}Xe released from the ANSTO facilities, we examine the transport for release of 3.18×10^{13} Bq on November 2, 2010. This was the largest of the daily releases in the data set. A snapshot of the extent of the plume ten days after the release is shown in Figure 9. The lowest concentration contour shown on the plot is 0.01 mBq/m^3, which is an order of magnitude below currently detectable concentrations. No radioactive decay is applied in this plot. Application of radioactive decay for ^{133}Xe, which has a half-life of about 5.24 days, would lower these concentrations by nearly a factor of 4.

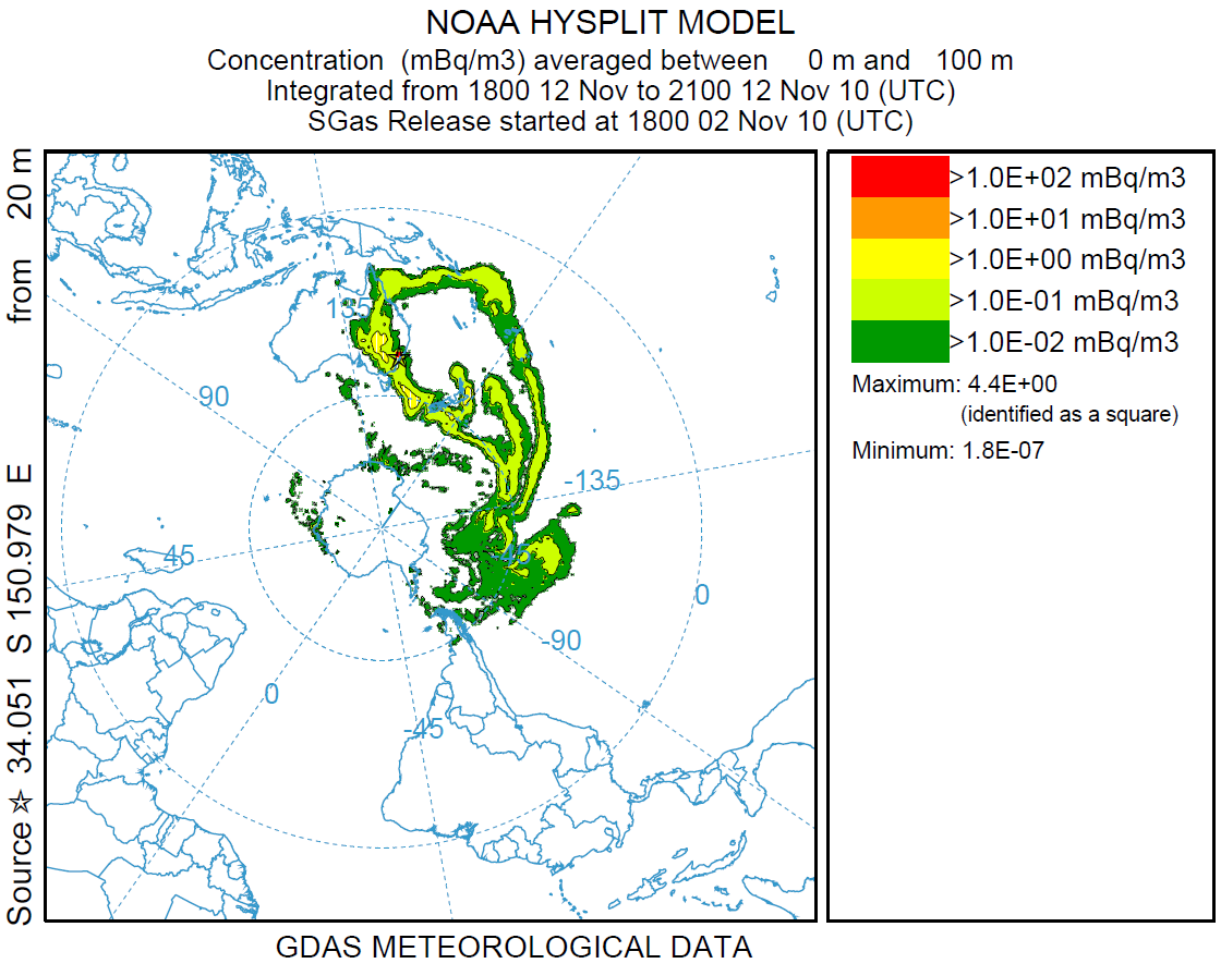

Figure 9. Modeled ^{133}Xe concentrations ten days after a release of 3.18×10^{13} Bq on November 2, 2010, from the ANSTO facilities. No radioactive decay is used.

3.2 Predicted Concentrations Using ANSTO Releases

The suite of model runs covered the time period from November 2008 through February 2012; a total of 1162 days. We calculated the percent of days the modeled concentrations were above 0.3 mBq/m^3 at each of the IMS locations with noble gas samplers We chose this particular concentration limit because it was the upper 95% of the suite of calculated MDC's, and thus it is likely that a station would report this concentration as a detection of ^{133}Xe. The results are shown in Figure 10. Most of the "detections" occur in Australia and New Zealand. The station identified as CLX19 (see Figure 1) is about half-way between New Zealand and South America.

Even though the other IMS radionuclide sampling locations do not have noble gas samplers, we include an expanded version of Figure 10 that considers concentrations at all IMS radionuclide sampling locations. Location 35 is assumed to be located in the country of India. These results are shown in Figure

11. We note that the modeled plume stays in the southern hemisphere and occasionally it travels as far as South America in detectable concentrations.

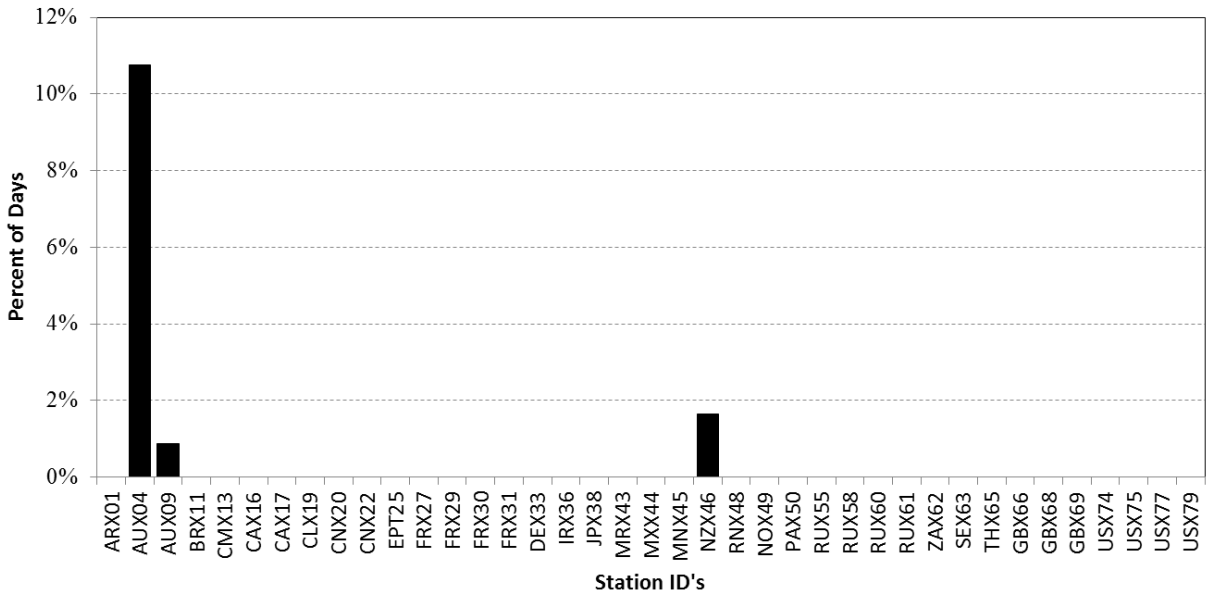

Figure 10. Percent of days that modeled ^{133}Xe concentrations were above 0.3 mBq/m^3 at IMS locations with noble gas samplers given the historical releases from the ANSTO facilities.

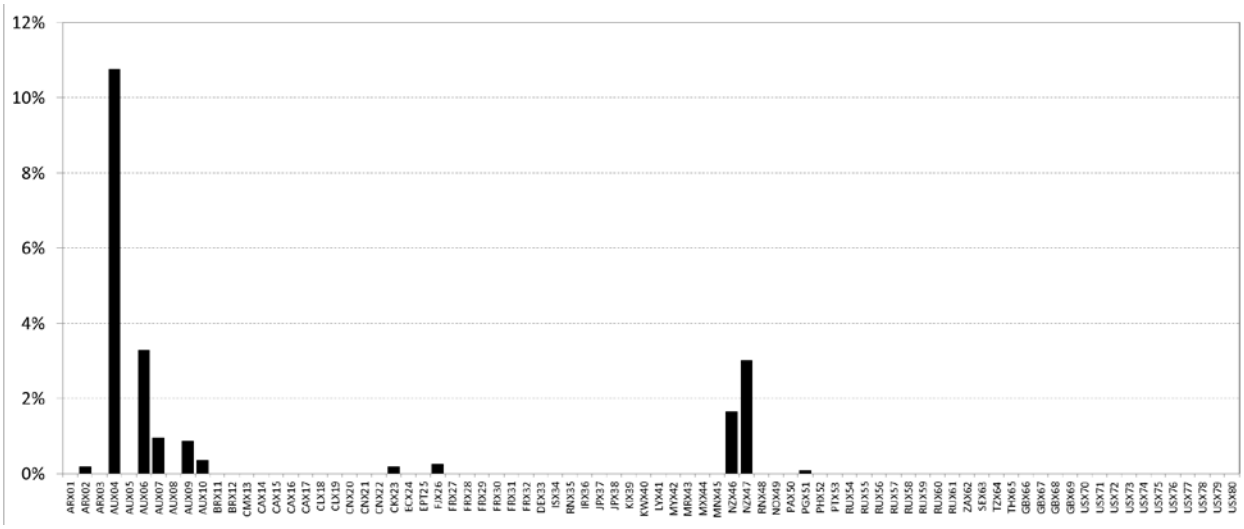

Figure 11. Percent of days that modeled ^{133}Xe concentrations were above 0.3 mBq/m^3 at all IMS radionuclide locations given the historical releases from the ANSTO facilities.

We also considered the match between IMS sampled data and the modeled concentrations for three sampling locations. A comparison of the sampled concentrations with modeled concentrations for the IMS station (AUX04) in Melbourne, Australia, is shown in Figure 12. The modeled concentrations are daily average concentrations, thus we have averaged the nominal two IMS samples per day to obtain a daily value. We only include measured concentrations in the plot that pass quality criteria. We only plot modeled data for days with valid measured data.

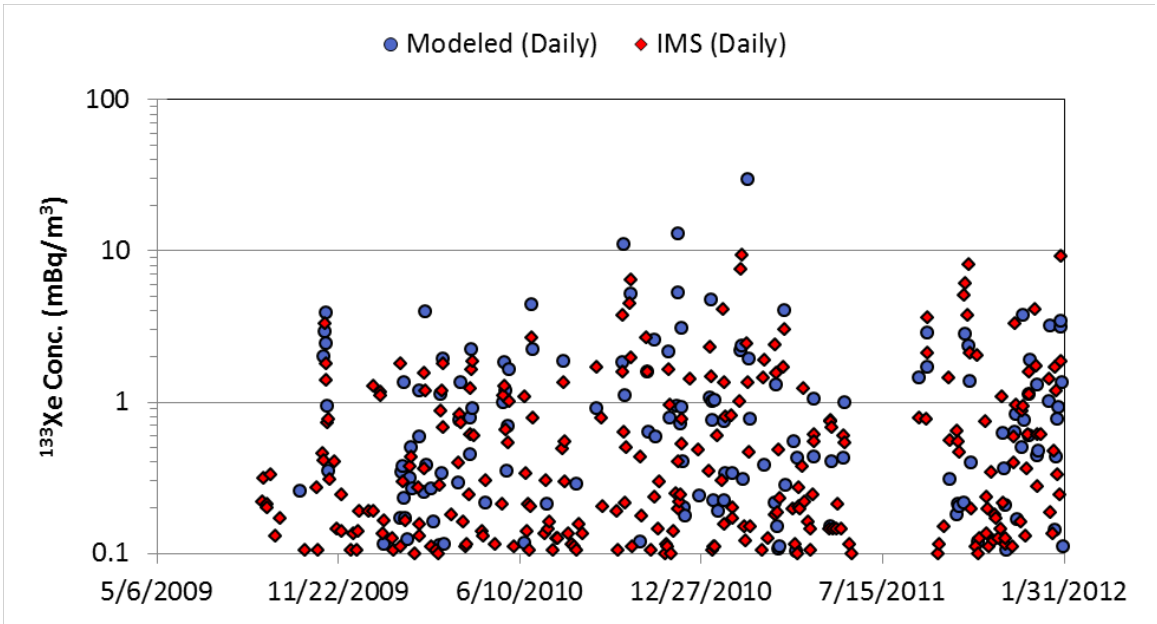

Figure 12. Time history of modeled and sampled concentrations for the IMS station (AUX04) in Melbourne, Australia, given the ^{133}Xe historical releases from the ANSTO facilities.

We plot all modeled concentrations against the daily average sampled concentrations in Figure 13 for sampled concentrations that meet or exceed 0.1 mBq/m^3.

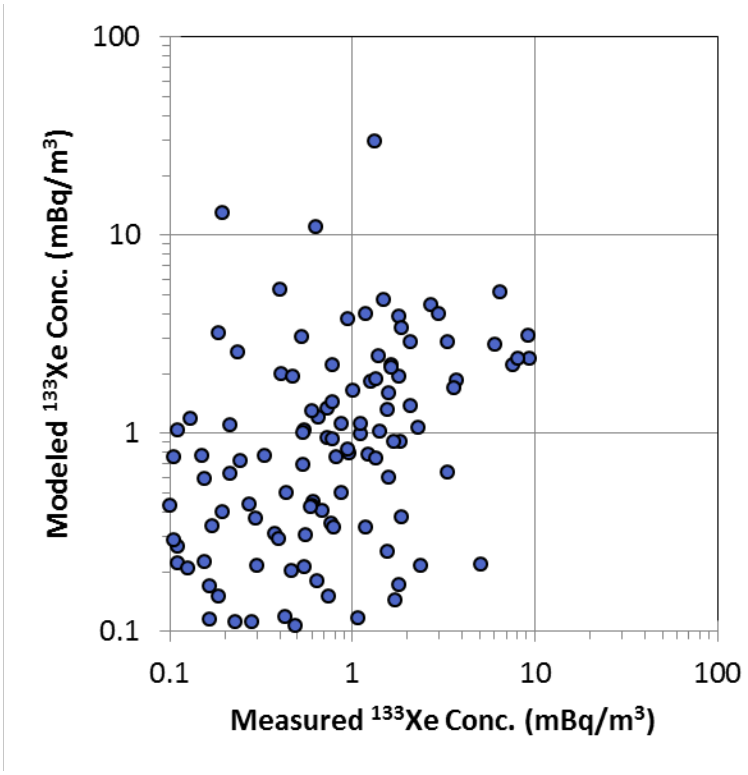

Figure 13. Comparison of modeled concentrations with sampled concentrations for the IMS station (AUX04) in Melbourne, Australia, given the ^{133}Xe historical releases from the ANSTO facilities.

Each sampled value has a calculated minimum detectable concentration. We calculated a binary measure for the comparison. A "match" can occur in two ways. First, the sampled value and the modeled concentration are both below the specific sample MDC. Second, the sampled value and the modeled concentration are both above the specific sample MDC. Other data combinations indicate a mismatch. Using this simple measure, 82% of the modeled concentrations for Melbourne (AUX04) match with the sampled concentrations, in the sense that they correctly identify days with detectable concentrations and days with concentrations below detection levels. Of the 18% of the dates resulting in mismatches, the model is higher than the sampled concentrations 26% of the time.

A comparison of the sampled concentrations with modeled concentrations for the IMS station (AUX09) in Darwin, Australia, is shown in Figure 14. The IMS data are converted to daily averages in this plot. We only plot modeled data for the days with valid sampled data. Using the simple matching measure, 33% of the modeled concentrations match with the sampled concentrations, in the sense that they correctly identify detections and concentrations below detection levels. Of the 67% of the dates resulting in mismatches, the model is lower than the sampled concentrations 100% of the time. We plot all modeled concentrations against the daily average sampled concentrations in Figure 15 for sampled concentrations that meet or exceed 0.1 mBq/m^3.

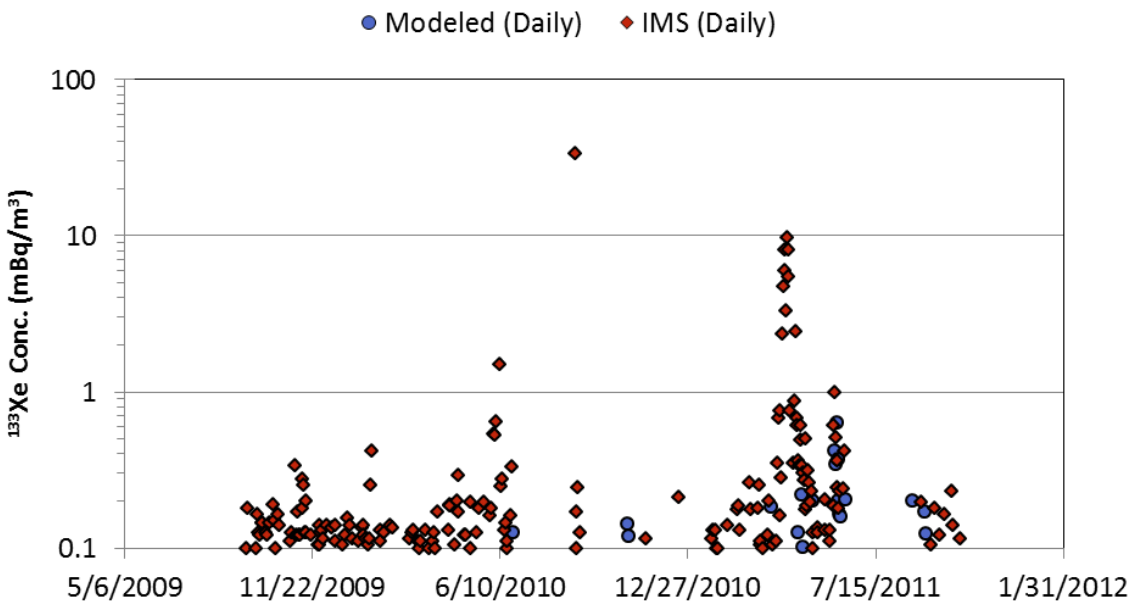

Figure 14. Time history of modeled and sampled concentrations for the IMS station (AUX09) in Darwin, Australia, given the ^{133}Xe historical releases from the ANSTO facilities.

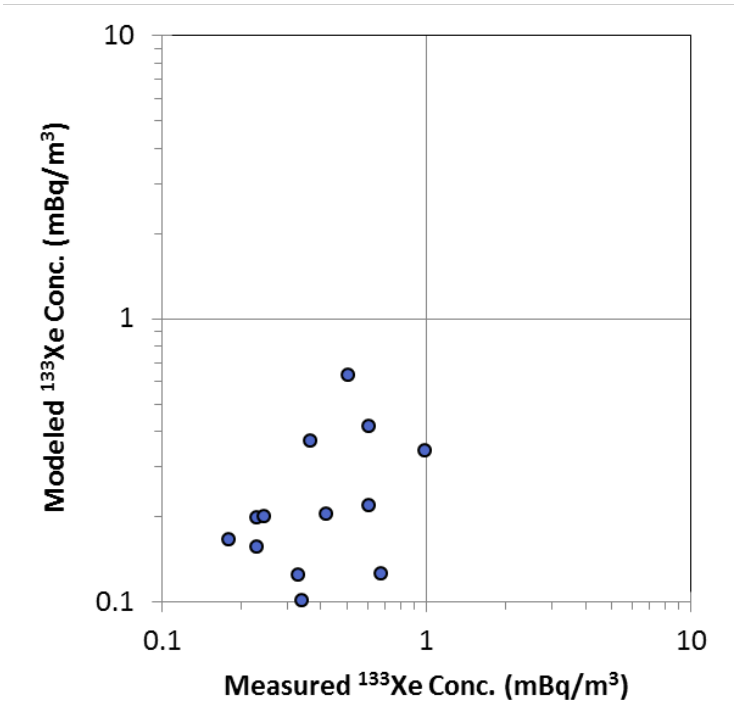

Figure 15. Comparison of modeled concentrations with sampled concentrations for the IMS station (AUX09) in Darwin, Australia, given the ^{133}Xe historical releases from the ANSTO facilities.

A comparison of the sampled concentrations with modeled concentrations for the IMS station (NZX46) in Chatham Island, New Zealand, is shown in Figure 16. The IMS data are not converted to daily averages in this plot. We only plot modeled data for the days with valid sampled data. Using the simple matching measure, 73% of the modeled concentrations match with the sampled concentrations, in the sense that they correctly identify detections and concentrations below detection levels. Of the 37% of the dates resulting in mismatches, the model is lower than the sampled concentrations 100% of the time.

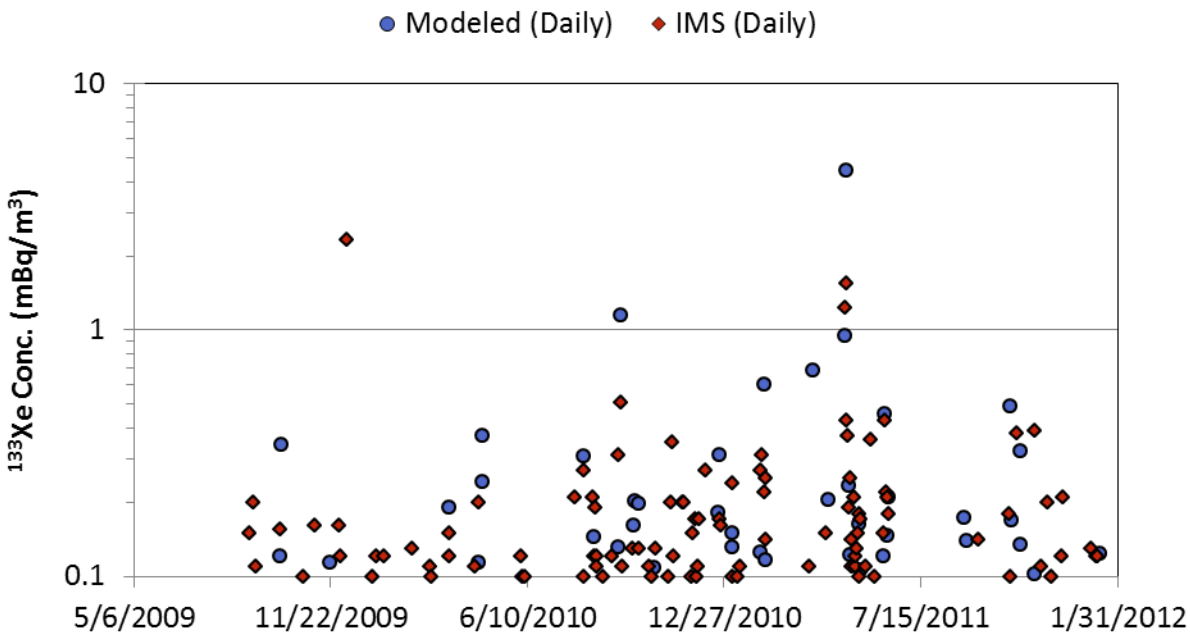

Figure 16. Time history of modeled and sampled concentrations for the IMS station (NZX46) in Chatham Island, New Zealand, given the ^{133}Xe historical releases from the ANSTO facilities.

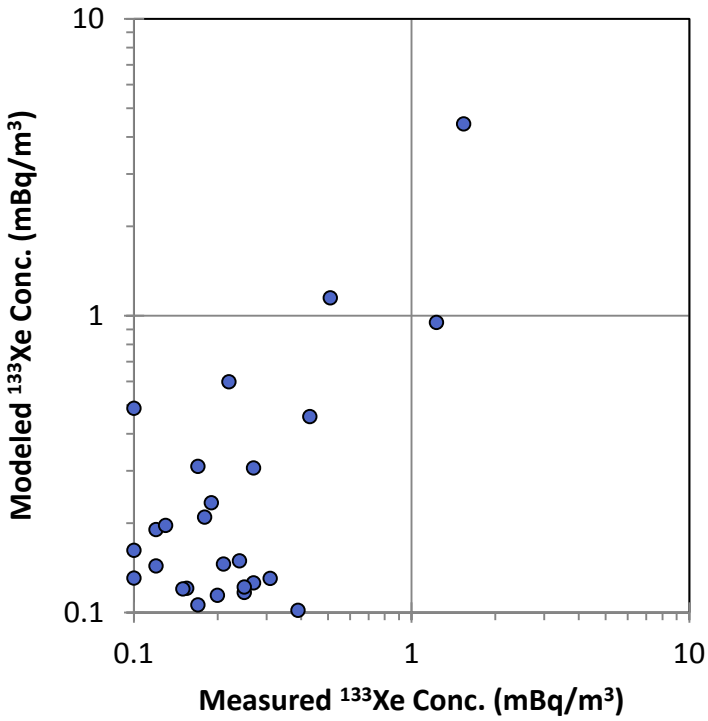

Figure 17. Comparison of modeled concentrations with sampled concentrations for the IMS station (NZX46) in Chatham Island, New Zealand, given the ^{133}Xe historical releases from the ANSTO facilities.

3.3 Analysis of Alternate Arrival Times

As shown in Figure 5, releases are not continuous throughout the day. The transport runs use daily release totals, and the totals are adjusted from local time to UTC because the meteorological data are use a UTC time basis. In addition, the post-processing program used in this analysis compute daily concentrations from the atmospheric transport runs. The samplers all use 12-hour samples, thus, they yield two samples during a 24 hour period. In addition, the actual 24-hour period on the modeled concentration can differ from two 12-hour sampling periods at a specific location. Thus, the potential for time mismatches on plume arrival exists in two ways. One way is that the meteorological data do not accurately represent local conditions. The second is simply due to the different timing used in the analysis steps. The results in Figure 18 show modeled and measured concentrations for AUX04 matching the best of two measured concentrations in a day with best modeled values at adjacent times. This simple analysis shows that the time of arrival of a modeled plume may vary by a day from the actual plume arrival.

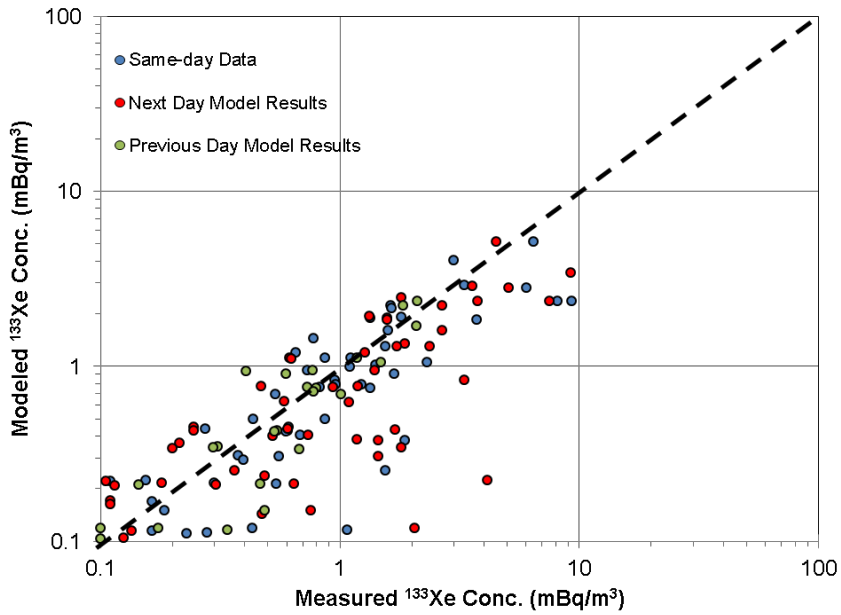

Figure 18. Best neighbor analysis with time offset for concentrations for the IMS station (AUX04) in Melbourne, Australia, given the ^{133}Xe historical releases from the ANSTO facilities.

A more detailed look at the same date is provided in Figure 19 for the simple binary matching algorithm, even for samples below the reported minimum detectable concentration. The nearest neighbor time correction improves the accuracy of the comparison.

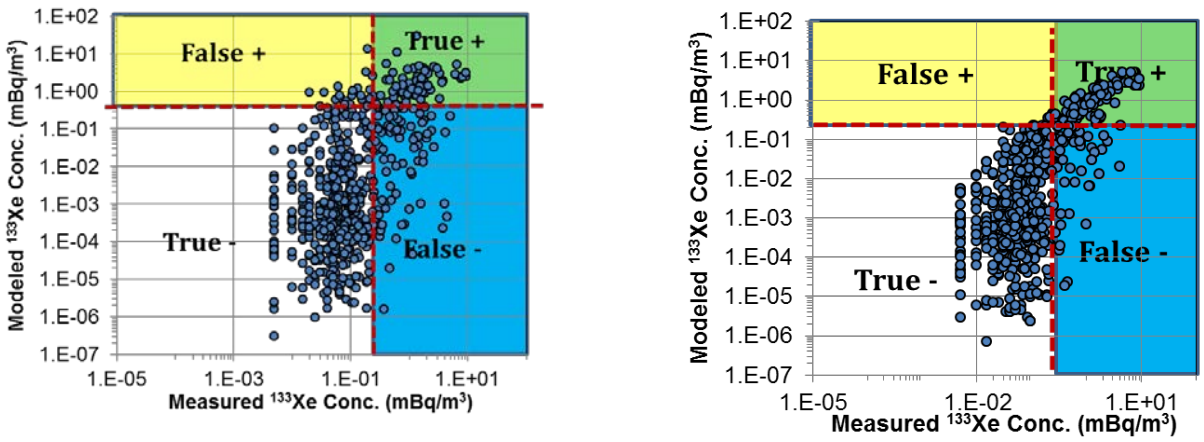

Figure 19. Binary matching results for offset for concentrations for the IMS station (AUX04) in Melbourne, Australia. Left pane provided same day results. Right pane shows nearest neighbor results.

The improvements in the results that are shown in Figure 19 are quantified in Table 1. The entries in the table are the fraction of the measured values that fallinto different classifications using the binary matching approach.

Table 1. Probabilities of model-measurement detection agreements for the IMS station (AUX04) in Melbourne, Australia.

Category	Same Day	Closest Neighbor
True-Positive	0.68	0.93
True-Negative	0.88	0.91
False Positive	0.32	0.07
False-negative	0.12	0.09

The nearest neighbor matching approach was extended to the three IMS noble gas stations closest to the ANSTO facilities. Results for detection predictions are provided in Figure 20 and results for non-detections are provided in Figure 21.

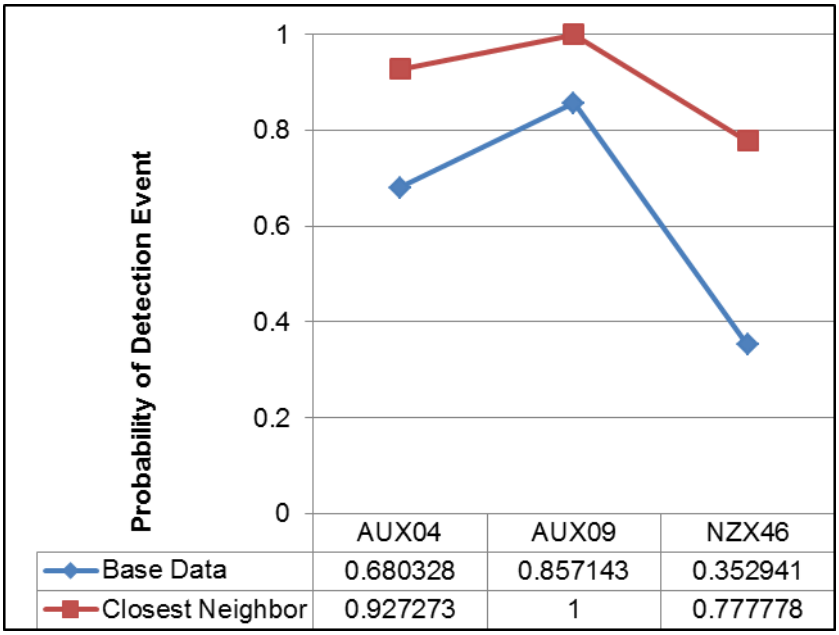

Figure 20. Successful detection predictions of same day model results versus closest neighbor data for the three IMS noble gas stations closest to the ANSTO facilities.

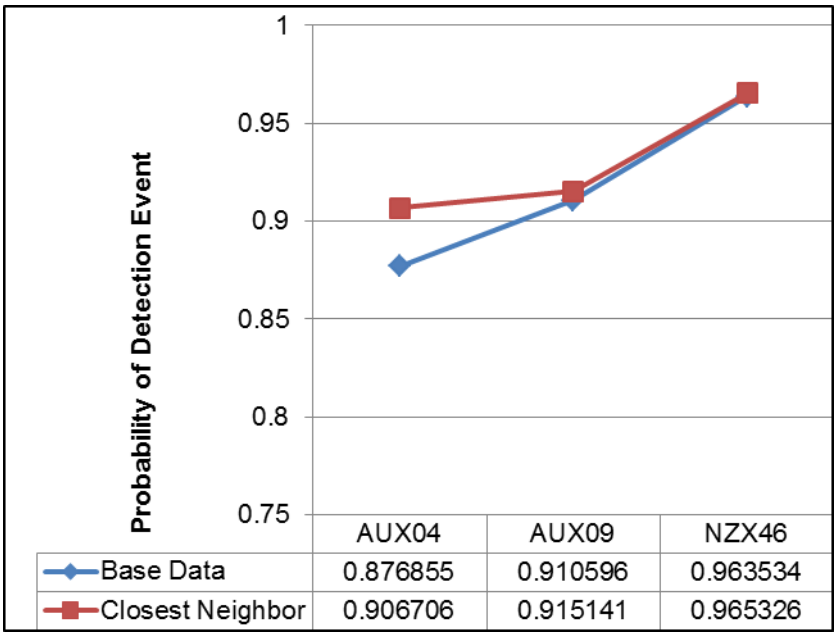

Figure 21. Successful non-detection predictions of same day model results versus closest neighbor data for the three IMS noble gas stations closest to the ANSTO facilities.

3.4 Other Potential Source Terms

The results for Darwin, Australia (AUX09), and Chatham Island, New Zealand (NZX46), indicate that mismatches between measured and model concentrations always occur with modeled concentrations being lower than the measured concentrations. This mismatch suggests that one or more other facilities in the southern hemisphere may be releasing ^{133}Xe. A figure showing the locations of worldwide nuclear power plants and southern hemisphere medical isotope production facilities is provided in Figure 22.

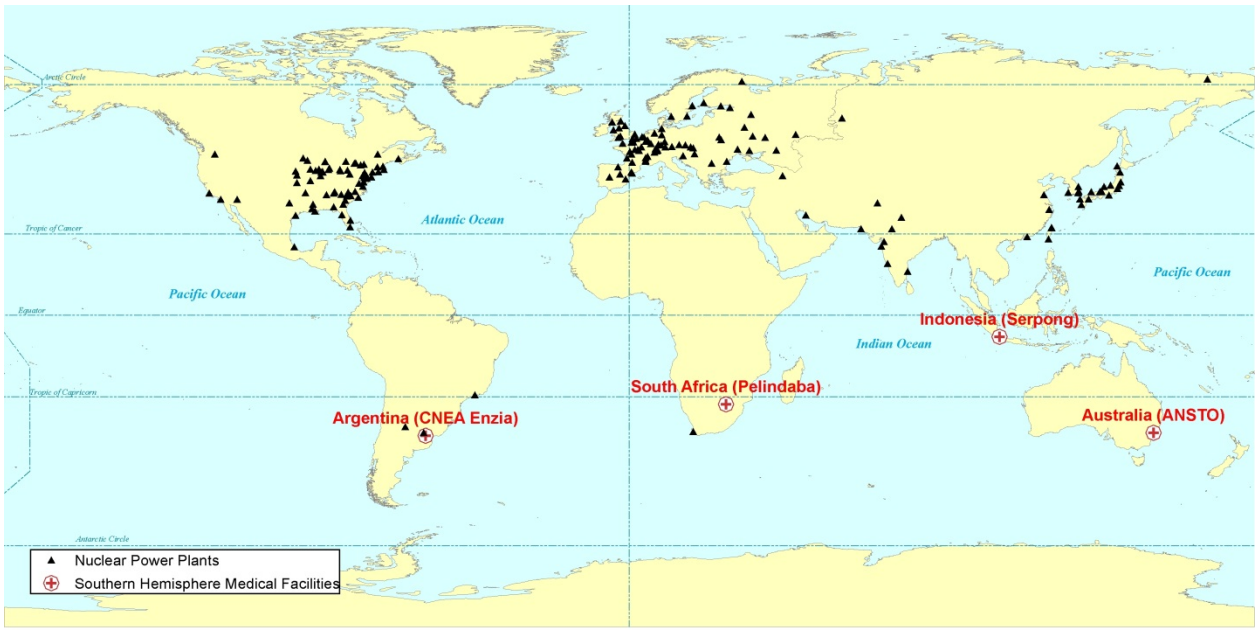

Figure 22. Worldwide nuclear power plant locations and southern hemisphere medical isotope production facilities.

The prevailing wind direction from the medical isotope production facility in Indonesia indicates that releases could routinely reach the IMS samplers in Darwin, Australia and Chatham Island, New Zealand. The Serpong medical isotope production facility has the capacity to produce 100 6-day Ci of ^{99}Mo per week (personal communication), but some news reports indicate they are seeking to raise the production to 900 6-day Ci of ^{99}Mo per week (Prasetyo 2012).). If there are 100 Ci (3.7×10^{12} Bq) of ^{99}Mo remaining six days after being packaged for distribution, then at least 1.68×10^{13} Bq of ^{99}Mo was present at the time of packaging. Dissolution of the uranium targets, chemical separation of the ^{99}Mo and packaging of the final product can take several days, although this time can vary widely from facility to facility. If the processing and packaging steps take three days, then at least 3.58×10^{13} Bq of ^{99}Mo was present when the targets entered the dissolution step. If these steps take six days, then at least 7.64×10^{13} Bq of ^{99}Mo was present when the targets entered the dissolution step. It is reasonable to make the assumption that as much ^{133}Xe is produced in the reactor as ^{99}Mo (Chadwick et al. 2011). It is reasonable to make the assumption that as much ^{133}Xe is produced in the reactor as ^{99}Mo (Chadwick et al. 2011). We average the implied weekly ^{99}Mo inventory over the time period from 3 to 6 days of processing, obtaining a value of 5.44×10^{13} Bq and then convert it to a constant daily release amount of 7.8×10^{12} Bq of ^{133}Xe

The facility in South Africa is estimated to release an average of 1.3×10^{13} Bq of ^{133}Xe per day (Saey 2009). In addition, the medical isotope production facility in Argentina has a capacity to process 600 6-day Ci of ^{99}Mo per week (OECD 2010). If they average only 1/6th of their rated capacity, they can also release on the order of 5.44×10^{13} Bq Bq of ^{133}Xe per week.

We considered the effect of the three additional medical isotope production locations with the assumption of releases of the same amount every day. Examination of the daily release data for ANSTO shows that a constant release assumption is a crude approximation, but the approximation probably can't be improved

without access to stack release data, if such even data exist. Also, we don't have access to data that would tell us when the separations plant is not in operation.

The three sampling locations (AUX04, AUX09 and NZX46) have 2,139 valid sampling data (daily average values from IMS samplers) over this time period. We use the historical releases from ANSTO and select the constant release values from the other three facility locations that minimize an objective function. We chose the objective function to be the sum of squared differences between the modeled concentrations and the sampled concentrations. For this exercise, we set negative IMS concentration estimates to zero. The best fitting constant releases 1.3×10^{14} Bq of ^{133}Xe per week for Argentina, 1.1×10^{14} Bq of ^{133}Xe per week from South Africa and 2.7×10^{12} Bq of ^{133}Xe per week from Indonesia.

A comparison of the sampled concentrations with modeled concentrations for the IMS station (AUX04) in Melbourne, Australia, is shown in Figure 23 for the releases from all four facilities. The modeled concentrations are daily average concentrations, thus we have averaged the nominal two IMS samples per day to obtain a daily value. We only plot modeled data for days with valid measured data. A visual comparison with Figure 12 shows that more days have modeled concentrations in the visible range on this plot.

We plot all modeled concentrations against the daily average sampled concentrations in Figure 24 for sampled concentrations that meet or exceed 0.1 mBq/m^3. This plot also more matches between modeled and sampled data, mostly in the range of concentrations below 1.0 mBq/m^3.

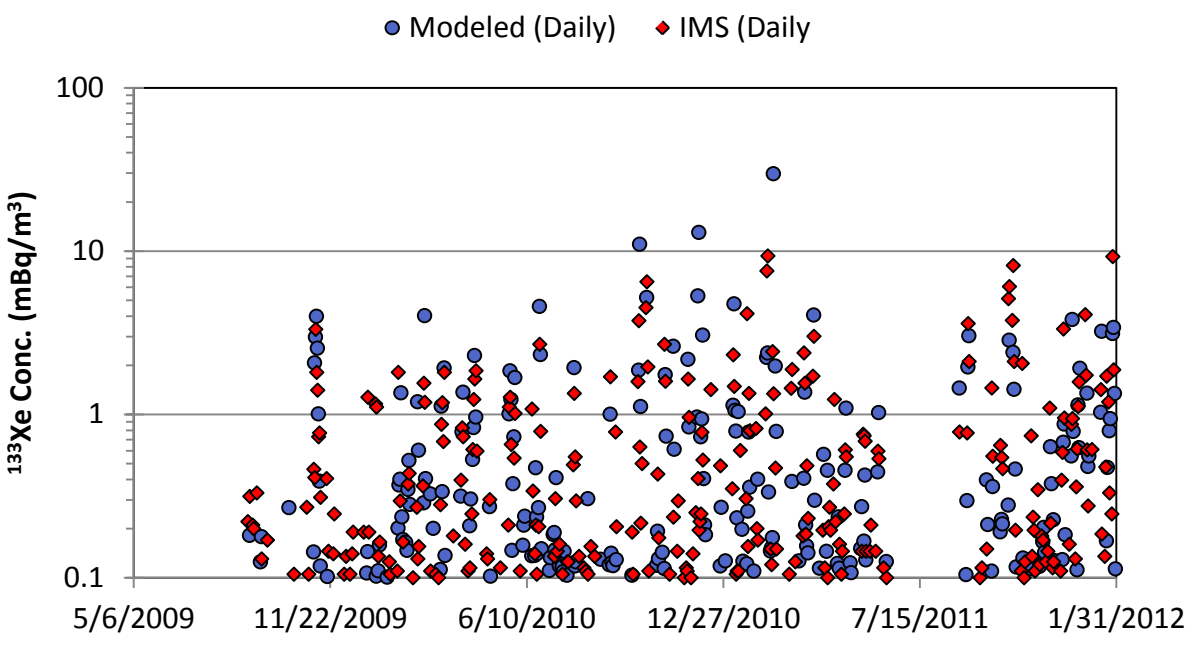

Figure 23. Time history of modeled and sampled concentrations for the IMS station (AUX04) in Melbourne, Australia, given the ^{133}Xe historical releases from the ANSTO facilities and estimated releases from Argentina, South Africa and Indonesia.

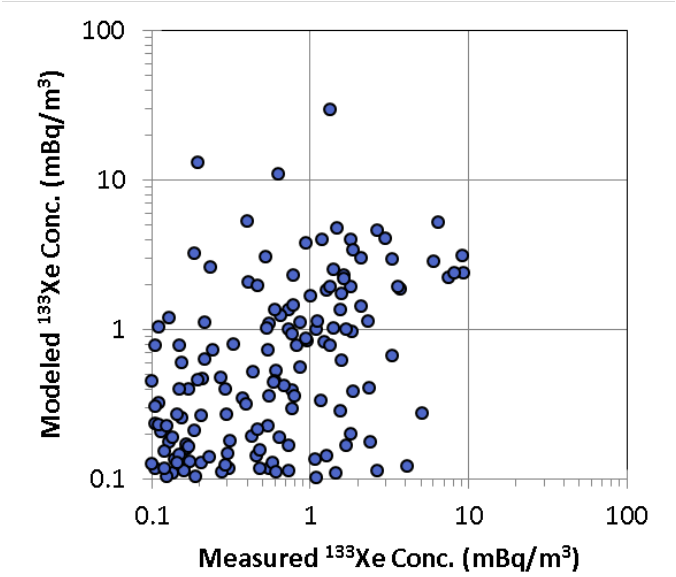

Figure 24. Comparison of modeled concentrations with sampled concentrations for the IMS station (AUX04) in Melbourne, Australia, given the ^{133}Xe historical releases from the ANSTO facilities and estimated releases from Argentina, South Africa and Indonesia.

A comparison of the sampled concentrations with modeled concentrations for the IMS station (AUX09) in Darwin, Australia, is shown in Figure 25 using the expanded set of source terms. Again, the additional source terms improve the comparison of modeled and sampled concentrations for days with low measured concentrations.

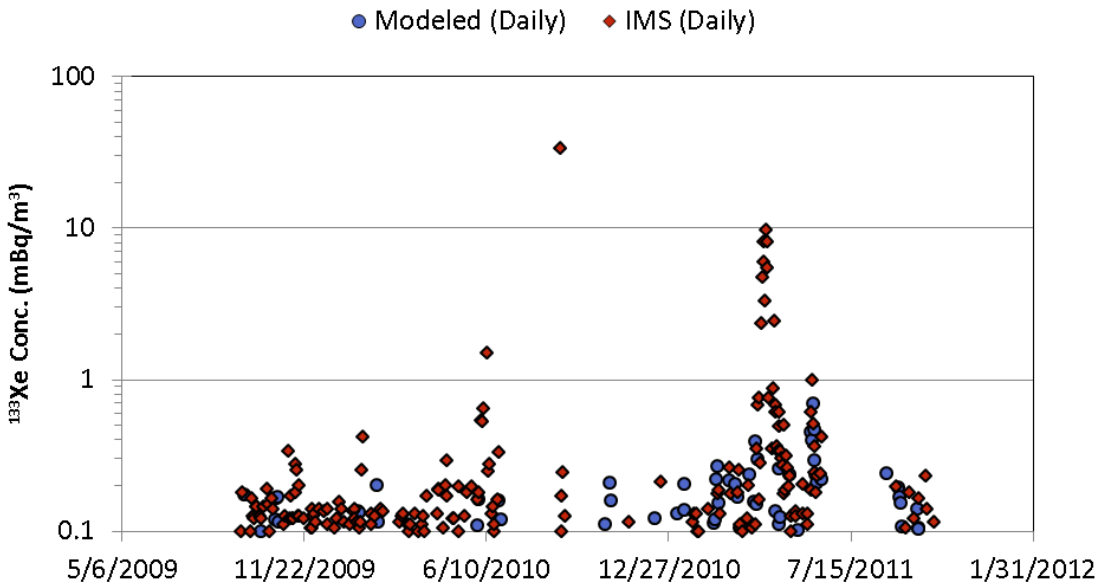

Figure 25. Time history of modeled and sampled concentrations for the IMS station (AUX09) in Darwin, Australia, given the ^{133}Xe historical releases from the ANSTO facilities.

A different measure of the quality of the modeling relative to the measurements is to examine the fraction of days the model predicts detectable concentrations against the historical data. Results for this simple measure are provided in Table 2. We start with the historical percentages. The historical percentages include all concentration estimates that pass quality checks, so many of the concentrations are below the MDC. We then calculated the percentages using only the historical ANSTO releases (Case 1). These results seem to underestimate sampled concentrations at AUX09, and slightly underestimate them at the other two locations. In case 2 we include the nominal releases discussed previously from the other three medical isotope production facilities in the southern hemisphere. These releases improve the match at AUX04, but seem to overestimate the higher concentrations at AUX09. In case 3, we use the historical release values for ANSTO and the best fit values for the other three facilities. It is interesting that this case does more poorly at AUX09 than the nominal release case. In case 4 we allow a constant multiplier on the historical ANSTO releases when we fit the best estimate releases. In case 5, we consider a solution with historical release from ANSTO and modified constant source terms from the other facilities. In this case, we select the approximate releases to match the fraction of days with concentrations above thresholds. This cases results in estimates releases of 2.0×10^{14} Bq of ^{133}Xe per week for Argentina, 2.2×10^{14} Bq of ^{133}Xe per week from South Africa and 1.1×10^{13} Bq of ^{133}Xe per week from Indonesia.

Table 2. Comparison of the percent of days measured and modeled concentrations of 133Xe are above specified concentrations at three southern hemisphere IMS noble gas samplers.

Data Configuration	Threshold Value	Threshold Value
IMS Historical Data	0.3 mBq/m^3	0.1 mBq/m^3
AUX04	17.3	35.8
AUX09	6.2	32.2
NZX46	1.8	14.1
Case 1: Only Historical Release at ANSTO		
AUX04	13.0	18.2
AUX09	0.7	3.1
NZX46	1.6	5.7
Case 2: Historical Release at ANSTO and Nominal (Constant Source) Releases at Argentina, South Africa and Indonesia		
AUX04	13.7	22.8
AUX09	15.5	24.5
NZX46	1.6	7.4
Case 3: Historical Release at ANSTO and Best Fit (Constant Source) Releases at Argentina, South Africa and Indonesia		
AUX04	14.1	28.4
AUX09	0.8	9.3
NZX46	1.6	9.0
Case 4: Best Fit Scaled Historical Release at ANSTO with Best Fit (Constant Source) Releases at Argentina, South Africa and Indonesia		
AUX04	12.9	52.2
AUX09	3.6	26.8
NZX46	1.4	20.8
Case 5: Historical Release at ANSTO with Modified (Constant Source) Releases at Argentina, South Africa and Indonesia		
AUX04	16.1	41.0
AUX09	6.2	27.2
NZX46	2.1	16.1

3.5 Detailed Analysis of One Short Detection Sequence

Several detections of ^{133}Xe at the IMS station in Melbourne, Australia, (AUX04) in November and December, 2008, and January, 2009, have been linked to the ANSTO facility through atmospheric modeling (Tinker et al. 2010). They used an atmospheric transport with higher resolution meteorological data than we used in this analysis.

As a corroborating exercise, we modeled releases from the ANSTO facilities between 1800 (UTC) on 12/9/2008 and 2100 on 12/12/2008 and compared them to measured data in Melbourne (AUX04). We divided the source term into 3-hour intervals and ran separate models for each interval. The model used

3-hour meteorological data archived on a 1° grid, but we used a more finely resolved (0.1°) concentration grid. The ^{133}Xe release data collected on 15-minute time intervals for this time period were summed into the appropriate 3-hour release period. The comparison of the measured values and the modeled values for the same time period are provided in Table 3. This example shows a reasonable match between measured and modeled concentrations using the forward model runs. We did not attempt to estimate any contribution to the modeled value from release at the other three production facilities.

Table 3. Comparison of measured and modeled concentrations of ^{133}Xe at Melbourne (AUX04) for releases from ANSTO facilities between 12/9/2008 and 12/12/2008.

Date and Time (UTC) Collection Start (12 hour collection)	**Measured Value mBq/m^3**	**Modeled Value mBq/m^3**
12/11/08 19:38	2	1.17
12/12/08 7:38	1.6	3.19
12/12/08 19:38	0.4	0.65

We then set aside the measured release data and used the dilution factors from the 18 higher resolution ATM runs to estimate the releases from the ANSTO facilities that would yield the measured values. The release estimate was generated by minimizing the sum of squares between the measured concentrations and the modeled concentrations. The minimization technique varied the amount released during each of the 18 time periods and assigned nonzero releases to only two time periods. Those releases were 4.42×10^{12} Bq at 0600 on the 9th and 1.23×10^{11} Bq at 2100 on the 9th, for a combined release of 4.54×10^{12} Bq. The sum of historical releases from the facility that has some influence on these measurements, given the wind direction, is about 2.3×10^{12} Bq. Thus, the model provides a reasonable estimate of the total release associated with these measurements. The measured and modeled concentrations are shown in Figure 26 and the released quantities are shown in Figure 27. Given that there are only three measured values, one would not expect to estimate nonzero release quantities for every 3-hour period in the model.

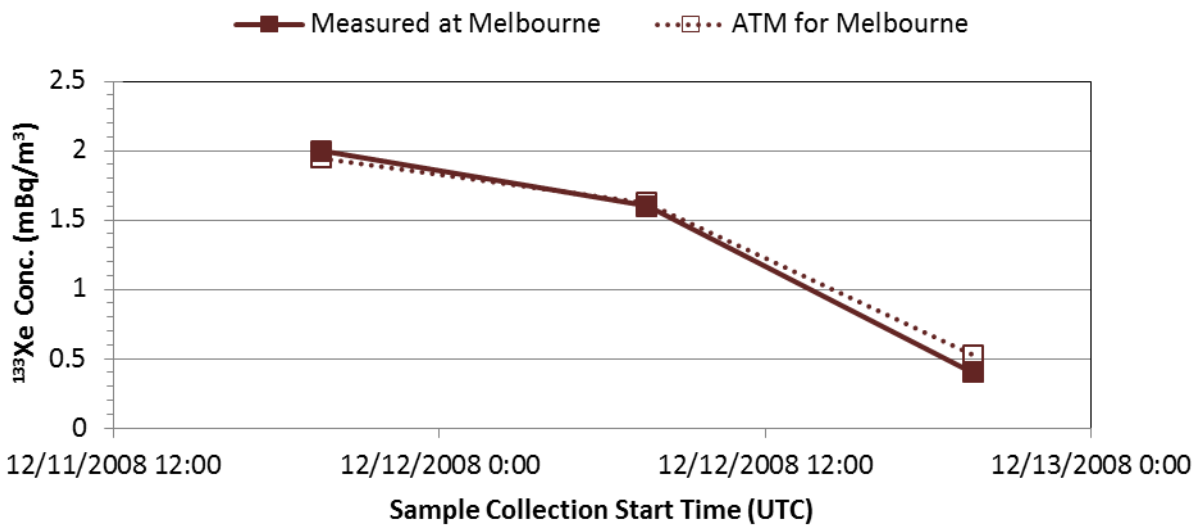

Figure 26. Comparison of measured and modeled concentrations of ^{133}Xe at Melbourne (AUX04) for releases from ANSTO facilities between 12/9/2008 and 12/12/2008.

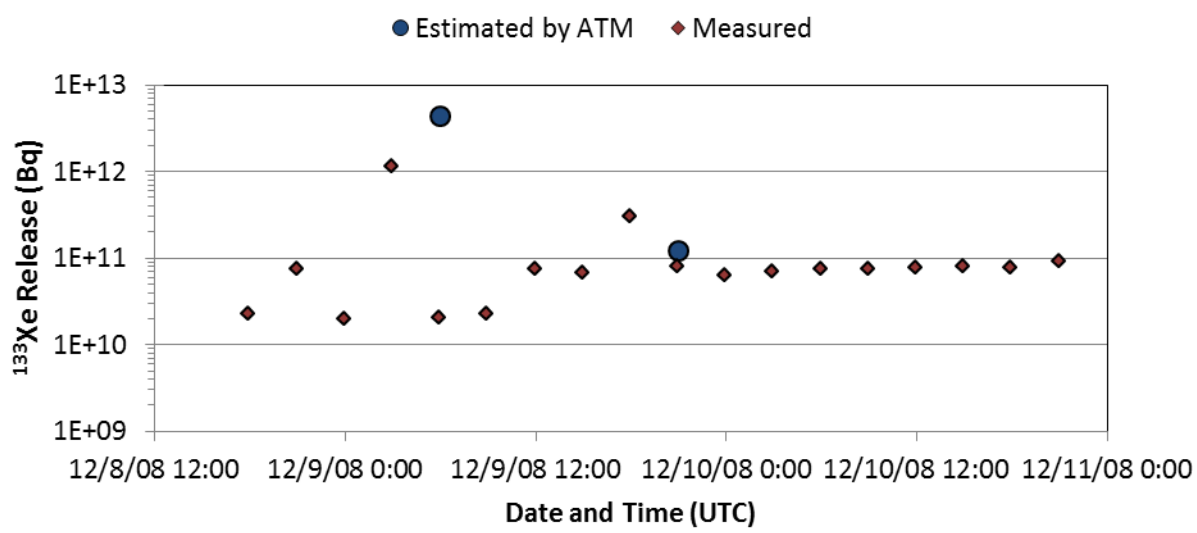

Figure 27. Comparison of estimated release quantities with stack release data for ANSTO facilities between 12/9/2008 and 12/12/2008.

4.0 Isotopic Analysis of ANSTO Stack Releases

Cluster analysis was applied to the 15-minute ANSTO medical isotope data. This analysis shows that there are clearly repeating processes occurring and that there are variations of the process throughout this period. Current measurements and an understanding of the models resulting from cluster analysis can be used to identify what "cluster" processes are occurring and what future measurements should be expected. This may be essential for IMS monitoring stations as medical isotope production increases and the number of Xenon measurements of significance increase for discerning between expected and unexpected Xenon measurements at IMS stations.

Cluster analysis methods achieve their utility by organizing data into groups where data within the group are more similar to data within the group than to data outside the group. This results in data reduction while preserving the original input space units. This is useful because the clusters can be analyzed with current methods to help characterize the cluster for identifying better semantic information about that cluster. In addition, clustering can be used to generate visual projections of data to assist the analyst. In the case of time series data, after the data have been analyzed with cluster analysis, each measurement can be labeled with the cluster identifier and a sequence of clusters can be identified that can be characterized as normal or unusual to form an anomaly detector.

A cluster analysis was performed on the ^{133}Xe, ^{135}Xe and ^{135m}Xe data. The results of a cluster analysis using 30 clusters is provided in Table 4.

Table 4. Isotopic structure of Xe using 30 clusters for the 15-minute data ANSTO release data.

Cluster	^{133}Xe	^{135}Xe	^{135m}Xe	Average distance in cluster	Number in cluster
V0	558.2	755.3	33.1	6.1	23
V1	7495.8	14.6	0.1	0.0	1
V2	56.0	51.9	53.6	1.7	108
V3	76.7	110.1	132.6	2.9	37
V4	17.8	8.7	6.6	0.3	587
V5	427.6	27.4	0.4	0.9	161
V6	126.9	80.4	2.2	0.8	314
V7	360.0	323.4	4.7	2.1	84
V8	61.3	75.6	88.2	2.0	67
V9	214.0	136.3	1.3	1.1	198
V10	1281.0	66.7	0.4	2.2	22
V11	40.0	18.4	0.7	0.2	1075
V12	266.3	363.6	88.0	4.6	37
V13	29.1	26.3	30.7	0.9	160
V14	153.5	203.2	220.1	4.5	31
V15	750.3	37.9	0.2	1.4	83
V16	15.7	6.8	0.6	0.1	4001
V17	80.5	42.1	1.0	0.5	489
V18	27.7	1.9	0.1	0.1	2955

Cluster	^{133}Xe	^{135}Xe	^{135m}Xe	Average distance in cluster	Number in cluster
V19	67.9	4.0	0.2	0.2	1132
V20	9.7	1.6	0.2	0.1	14129
V21	18664.7	132.4	0.2	36.1	2
V22	255.6	209.1	7.8	1.9	145
V23	502.4	495.9	6.4	3.0	45
V24	27.7	18.2	16.4	0.6	256
V25	143.5	7.8	0.2	0.3	555
V26	2401.7	46.3	0.1	2.7	8
V27	251.0	19.5	0.2	0.6	303
V28	333.7	465.5	336.3	10.0	7
V29	2.6	0.1	0.0	0.0	40374

Example isotopic information for five of the first six clusters identified in Table 4 is provided in Table 5. Cluster V1 is omitted because it consists of only a single data point.

Table 5. Example isotopic information for the five Xe clusters for the 30-cluster analysis of the 15-minute data ANSTO release data.

Cluster		Minimum	Maximum	Mean	St. Deviation	count
V0	^{133}Xe	0	1514.3	583.5	243.6	23
	^{135}Xe	0	1127.4	789.7	128.9	23
	^{135m}Xe	0	176.9	34.6	48.5	23
V2	^{133}Xe	0	640.8	56.6	73.7	108
	^{135}Xe	0	190.5	52.4	45.0	108
	^{135m}Xe	0	71.5	54.1	8.8	108
V3	^{133}Xe	0	204.1	78.8	47.0	37
	^{135}Xe	0	309.2	113.1	69.7	37
	^{135m}Xe	0	175.1	136.3	18.9	37
V4	^{133}Xe	0	86.7	17.9	13.0	587
	^{135}Xe	0	38.3	8.7	6.6	587
	^{135m}Xe	0	12.0	6.7	2.2	587
V5	^{133}Xe	0	604.2	433.0	65.5	161
	^{135}Xe	0	96.8	28.3	25.2	161
	^{135m}Xe	0	14.5	0.4	1.6	161

Because ^{135}Xe has a much shorter half-life than ^{133}Xe, the ratio of these two isotopes can be used to develop a simple process time ordering. The ratio of the mean concentration of these isotopes within clusters is provided in Table 6. Clusters V1, V21 and V26 were omitted because they have few (1 to 8 data) sample data in the cluster and they may represent outliers.

Table 6. Example time ordering of releases of cluster means based on $^{133}Xe/^{135}Xe$ ratios for the 30-cluster analysis of the 15-minute data ANSTO release data.

Ratio	Cluster
0.66	V3
0.71	V14
0.94	V28
0.99	V8
1.12	V12
1.34	V0
1.51	V23
1.56	V13
2.00	V7
2.26	V4
2.67	V24
3.05	V6
3.12	V17
3.22	V16
3.23	V11
3.33	V9
3.36	V2
3.45	V22
3.91	V20
4.53	V29
6.03	V27
6.24	V5
6.70	V18
7.51	V19
7.63	V25
7.69	V15
8.17	V10

A cluster transition diagram for the 30 cluster analysis is provided in Figure 28. This diagram illustrates the exchange of data between clusters.

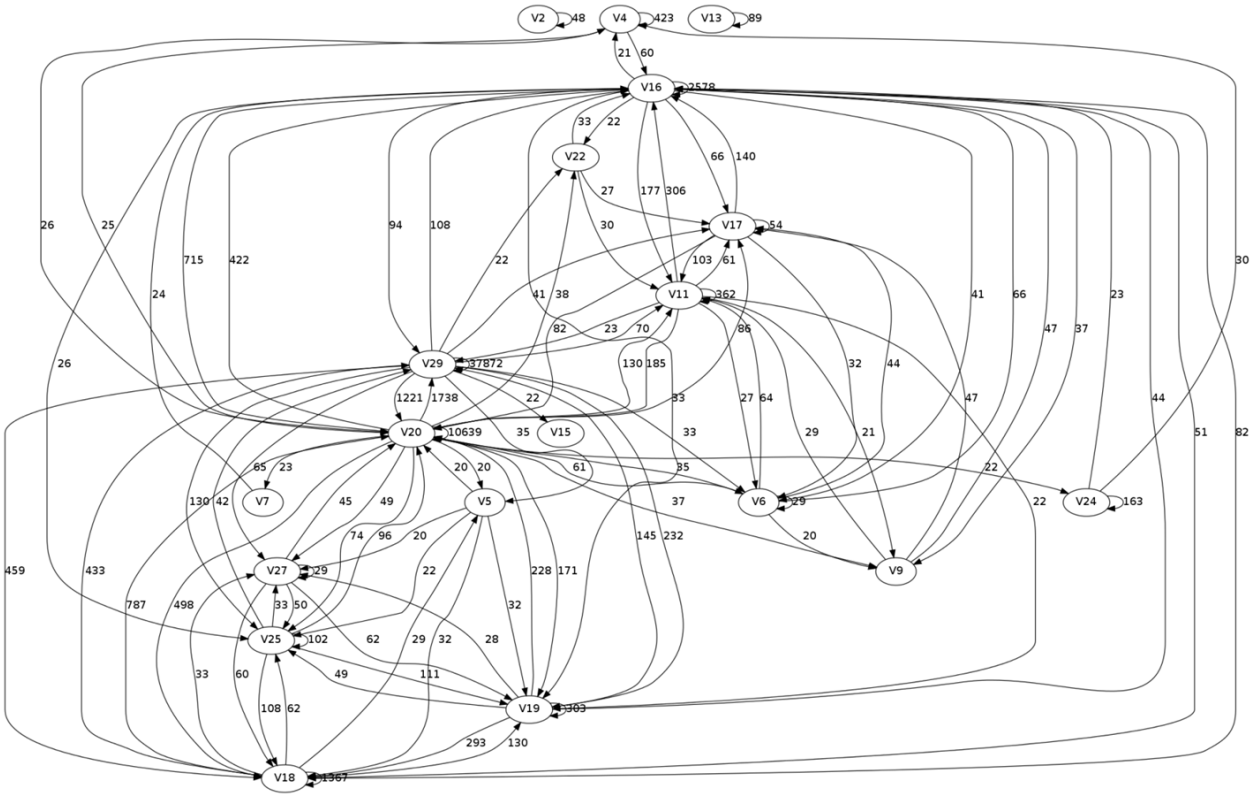

Figure 28. Cluster transitions for three isotopes of Xe using 30 clusters for the 15-minute data ANSTO release data.

Approximately half of the data samples ended up in cluster V29. Using the number of data values in each cluster (as shown in Table 4), one can put rough bounds on the isotopic ratios that results from most of the plant emissions. Such information might be useful in developing a typical signature for emission similar to the isotopic ratios studied for nuclear power plants and nuclear explosions (Kalinowski et al. 2010).

This analysis illustrates the complex isotopic structure of releases from many separate batches from a single processing plant. Discovering signatures in the isotopic data unique to medical isotope production would be useful in discriminating releases from those facilities from potential releases due to nuclear explosions. Clustering is one method available to gain insight during the signature discovery process. It is useful in summarizing massive amounts of raw data into semantically meaningful information. This information may be combined later with higher level analysis to support signature discrimination analyses.

5.0 Summary

We have combined historical release data of ^{133}Xe from ANSTO facilities with an atmospheric transport model to estimate the impact these releases have on noble gas samplers in the International Monitoring System. Historical data show concentrations of ^{133}Xe at or above 0.3 mBq/m^3 about 17% of the time at Melbourne. Modeled data suggest that releases from ANSTO heavily influence these measurements, but they do not explain all of the detections. The ANSTO releases also influence detections at Darwin, Australia, and Chatham Island, New Zealand, but to a lesser extent.

Any reasonable match of modeled with sampled data at these three sampling station also requires consideration of releases from medical isotope production facilities in Argentina, South Africa and Indonesia. We do not have release histories for these facilities, but the sampling data suggest releases of 2×10^{14} Bq of ^{133}Xe per week for Argentina, 2×10^{14} Bq of ^{133}Xe per week from South Africa and 1×10^{13} Bq of ^{133}Xe per week from Indonesia. Modeling of releases from these four southern hemisphere medical isotope production facilities can explain the frequency of ^{133}Xe detections.

A clustering algorithm applied to xenon isotopic data collected on a 15-minute frequency provides some insight into the isotopic mix in the releases. Such methods may be useful for developing potential release signatures unique to medical isotope production facilities.

6.0 References

ANSTO. 2012. *Nuclear Medicine*. Accessed on April 26, 2012, at http://www.ansto.gov.au/discovering_ansto/what_does_ansto_do/nuclear_medicine

Chadwick, MB, M Herman, P Obložinský, ME Dunn, Y Danon, AC Kahler, DL Smith, B Pritychenko, G Arbanas, R Arcilla, R Brewer, DA Brown, et al. 2011. "ENDF/B-VII.1 Nuclear Data for Science and Technology: Cross Sections, Covariances, Fission Product Yields and Decay Data." *Nuclear Data Sheets* 112(12):2887-2996, DOI:10.1016/j.nds.2011.11.002.

CTBT. 1996. *Text of the Comprehensive Nuclear-Test-Ban Treaty.* United Nations Office for Disarmament Affairs (UNODA), Status of Multilateral Arms Regulation and Disarmament Agreements, CTBT. Accessed on September 20, 2012, at http://www.ctbto.org/the-treaty/treaty-text/

CTBTO. 2011. *Ctbto Preparatory Commission Web Page.* Accessed on September 24, 2011, at http://www.ctbto.org/

Draxler, RR, and GD Hess. 1998. "An Overview of the Hysplit_4 Modeling System of Trajectories, Dispersion, and Deposition." *Aust. Meteor. Mag.* 47:295-308.

GDAS. 2012. *Downloadable Global Data Assimilation System Information Data Set Archive.* Air Resources Laboratory, National Oceanic and Atmospheric Administration. Accessed on April 2, 2012, at ftp://arlftp.arlhq.noaa.gov/pub/archives/gdas1/

HYSPLIT. 2011. *Air Resources Laboratory Hysplit Model.* Accessed on October 3, 2011, at http://www.arl.noaa.gov/documents/Summaries/HYSPLIT_FINAL.pdf (last updated March 2011).

Kalinowski, M, A Axelsson, M Bean, X Blanchard, T Bowyer, G Brachet, S Hebel, J McIntyre, J Peters, C Pistner, M Raith, A Ringbom, et al. 2010. "Discrimination of Nuclear Explosions against Civilian Sources Based on Atmospheric Xenon Isotopic Activity Ratios." *Pure and Applied Geophysics* 167(4):517-539, DOI:10.1007/s00024-009-0032-1.

Matthews, KM, TW Bowyer, PRJ Saey, and RF Payne. 2012. "The Workshop on Signatures of Medical and Industrial Isotope Production – Wosmip; Strassoldo, Italy, 1–3 July 2009." *Journal of Environmental Radioactivity* 110(0):1-6, DOI:10.1016/j.jenvrad.2012.01.012.

Matthews, KM, PRJ Saey, TW Bowyer, G Vandergrift, N Ramamoorthy, C Cutler, B Ponsard, R Mikolajczak, YM Tsipenyuk, LM Solin, D Fisher, K Ungar, et al. 2010. *Workshop on Signatures of Medical and Industrial Isotope Production - a Review.*PNNL-19294, Pacific Northwest National Laboratory, Richland, Washington.

OECD. 2010. *The Supply of Medical Radioisotopes. An Economic Study of the Molybdenum-99 Supply Chain.*, ISBN 978-92-64-99149-1, Nuclear Enercy Agency. Organisation for Economic Co-Operation and Development.

Prasetyo, B. 2012. *Dahlan Lirik Potensi Ekspor Radioaktif Ke China*. Tribune News. Accessed on September 25, 2012, at http://www.tribunnews.com/2012/03/28/dahlan-lirik-potensi-ekspor-radioaktif-ke-china

Saey, PRJ. 2009. "The Influence of Radiopharmaceutical Isotope Production on the Global Radioxenon Background." *Journal of Environmental Radioactivity* 100(5):396-406, DOI:10.1016/j.jenvrad.2009.01.004.

Saey, PRJ, M Auer, A Becker, E Hoffmann, M Nikkinen, A Ringbom, R Tinker, C Schlosser, and M Sonck. 2010. "The Influence on the Radioxenon Background During the Temporary Suspension of Operations of Three Major Medical Isotope Production Facilities in the Northern Hemisphere and During the Start-up of Another Facility in the Southern Hemisphere." *Journal of Environmental Radioactivity* 101(9):730-738, DOI:10.1016/j.jenvrad.2010.04.016.

Tinker, R, B Orr, M Grzechnik, E Hoffmann, P Saey, and S Solomon. 2010. "Evaluation of Radioxenon Releases in Australia Using Atmospheric Dispersion Modelling Tools." *Journal of Environmental Radioactivity* 101(5):353-361, DOI:10.1016/j.jenvrad.2010.02.003.

Wotawa, G, A Becker, M Kalinowski, P Saey, M Tuma, and M Zähringer. 2010. "Computation and Analysis of the Global Distribution of the Radioxenon Isotope ^{133}xe Based on Emissions from Nuclear Power Plants and Radioisotope Production Facilities and Its Relevance for the Verification of the Nuclear-Test-Ban Treaty." *Pure and Applied Geophysics* 167(4-5):541-557, DOI:10.1007/s00024-009-0033-0.

Pacific Northwest
NATIONAL LABORATORY

Proudly Operated by **Battelle** *Since 1965*

U.S. DEPARTMENT OF
ENERGY

902 Battelle Boulevard
P.O. Box 999
Richland, WA 99352
1-888-375-PNNL (7665)
www.pnl.gov